Novel Zirconium and Hafnium Complexes of Monoanionic Di-*N*,*N*′-chelating Pyridyl- and Quinolyl-1-azaallyl Ligands and Their Activity in Olefin Polymerization Catalysis

Berth-Jan Deelman,[†] Peter B. Hitchcock,[†] Michael F. Lappert,*[,†] Wing-Por Leung,[‡] Hung-Kay Lee,[‡] and Thomas C. W. Mak[‡]

The Chemistry Laboratory, University of Sussex, Brighton, BN1 9QJ, U.K., and Department of Chemistry, The Chinese University of Hong Kong, Shatin, New Territories, Hong Kong

Received October 13, 1998

The lithium complexes [Li{N(SiMe$_3$)C(R^1)C(R^2)(C$_5$H$_4$N-2)}]$_2$ (**1a**, **2a**, and **3a**) were each treated with MCl$_4$ to afford the racemic complexes [M{N(SiMe$_3$)C(R^1)C(R^2)(C$_5$H$_4$N-2)}$_2$Cl$_2$] (M = Zr, R^1 = Ph, R^2 = H (**1b**); M = Zr, R^1 = Bu^t, R^2 = H (**2b**); M = Hf, R^1 = Bu^t, R^2 = H (**2c**); M = Zr, R^1 = Ph, R^2 = SiMe$_3$ (**3b**)). Similarly, Li{N(SiMe$_3$)C(Ph)C(R)(C$_9$H$_6$N-2)} (**4a** and **5a**) afforded the racemic complexes [Zr{N(SiMe$_3$)C(Ph)C(R)(C$_9$H$_6$N-2)}$_2$Cl$_2$] (R = H (**4b**); R = SiMe$_3$ (**5b**)). X-ray structural analysis of **2b**, **2c**, and **3b** revealed that these complexes have C_2 octahedral geometries with their chloride ligands in *cis* positions. Molecular orbital calculations on model systems of the bis{3-(2-pyridyl)-1-azaallyl}zirconium system [Zr(LL)$_2$]$^{2+}$ (LL = [N(H)C(H)C(H)(2-C$_5$H$_4$N]) demonstrate that (i) the frontier orbitals are similar to those of [Zr(η^5-C$_5$H$_5$)$_2$]$^{2+}$ and (ii) the bis{3-(2-pyridyl)-1-azaallyl} ligand environment is more electron-donating, making the zirconium system less electrophilic. Conproportionation of ZrCl$_4$ with [Zr{N(SiMe$_3$)C(R^1)C(R^2)(C$_5$H$_4$N-2)}$_2$Cl$_2$] or [Zr{N(SiMe$_3$)C(Ph)C(SiMe$_3$)(C$_9$H$_6$N-2)}$_2$Cl$_2$] afforded the mono(1-azaallyl)zirconium complexes Zr{N(SiMe$_3$)C(R^1)C(R^2)(C$_5$H$_4$N-2)}Cl$_3$ (R^1 = Bu^t, R^2 = H (**2d**); R^1 = Ph, R^2 = SiMe$_3$ (**3d**)) and Zr{N(SiMe$_3$)C(Ph)C(SiMe$_3$)(C$_9$H$_6$N-2)}Cl$_3$ (**5d**), respectively. When activated with methylaluminoxane (MAO), these compounds were highly active in ethylene polymerization. Compound **3d** also showed modest activity in the polymerization of 1-hexene and the copolymerization of ethylene and 1-hexene.

Introduction

The continuing development of new spectator ligands in early transition metal chemistry, especially for group 4 metals, is stimulated by the search for new noncyclopentadienyl catalysts for α-olefin polymerization.[1] As a result, a range of new ligands has become available. Examples include polydentate Schiff bases,[2] benza- and alkylamidinates,[3] multidentate amides,[4] macrocyclic nitrogen ligands,[5] porphyrins, porphyrinogens,[6] and biphenoxy[7] ligands. However, relatively few of their derived metal complexes have had catalytic activities that can match those of the bis(cyclopentadienyl) systems.

Stimulated by the successful introduction of bulky *N*,*N*′-bis(trimethylsilyl)-*β*-diketiminato ligands (**a** and **b** in Figure 1) on zirconium[8] and the observation that some of the derived [Zr{*N*,*N*′-bis(trimethylsilyl)-*β*-diketiminato}Cl$_3$] complexes show high activity in catalytic α-olefin polymerization when combined with methylaluminoxane (MAO) as cocatalyst,[9] we designed novel

[†] University of Sussex.

[‡] The Chinese University of Hong Kong.

(1) For some recent reviews see: (a) Brintzinger, H. H.; Fischer, D.; Mülhaupt, R.; Rieger, B.; Waymouth, R. M. *Angew. Chem., Int. Ed. Engl.* **1995**, *34*, 1143. (b) Möhring, P. C.; Coville, N. J. *J. Organomet. Chem.* **1994**, *479*, 1. (c) Horton, A. D. *Trends Polym. Sci.* **1994**, *2*, 158. (d) Janiak, C. J. in *Metallocenes; Synthesis, Reactions and Applications*; Togni, A., Halteman, R. L., Eds.; Wiley-VCH: Weinheim, 1998; Vol. 2, Chapter 9. (e) Britovsek, G. J. P.; Gibson, V. C.; Wass, D. F. *Angew. Chem., Int. Ed. Engl.* **1999**, *38*, 429.

(2) (a) Tjaden, E. B.; Swenson, D. C.; Jordan, R. F.; Petersen, J. L. *Organometallics* **1995**, *14*, 371. (b) Corazza, F.; Solari, E.; Floriani, C.; Chiesi-Villa, A.; Guastini, C. *J. Chem. Soc., Dalton Trans.* **1990**, 1335. (c) Cozzi, P. G.; Floriani, C.; Chiesi-Villa, A.; Rizzoli, C. *Inorg. Chem.* **1995**, *34*, 2921, and references therein.

(3) (a) Herskovics-Korine, D.; Eisen, M. S. *J. Organomet. Chem.* **1995**, *503*, 307. (b) Flores, J. C.; Chien, J. C. W.; Rausch, M. D. *Organometallics* **1995**, *14*, 1827. (c) Gómez, R.; Duchateau, R.; Chernega, A. N.; Teuben, J. H.; Edelmann F. T.; Green, M. L. H. *J. Organomet. Chem.* **1995**, *491*, 153. (d) Roesky, H. W.; Meller, B.; Noltemeyer, M.; Schmidt, H.-G.; Scholz, U.; Sheldrick, G. M. *Chem. Ber.* **1988**, *121*, 1403. (e) Volkis, V.; Shmulinson, M.; Averbuj, C.; Lisovskii, A.; Edelmann, F. T.; Eisen, M. S. *Organometallics* **1998**, *17*, 3155. (f) Littke, A.; Sleiman, N.; Bensimon, C.; Richeson; D. S.; Yap, G. P. A.; Brown, S. J. *Organometallics* **1998**, *17*, 446.

(4) (a) Cloke, F. G. N.; Hitchcock, P. B.; Love, J. B. *J. Chem. Soc., Dalton Trans.* **1995**, 25. (b) Kol, M.; Schrock, R. R.; Kempe, R.; Davis, W. M. *J. Am. Chem. Soc.* **1994**, *116*, 4382. (c) Scollard, J. D.; McConville, D. H.; Rettig, S. J. *Organometallics* **1997**, *16*, 1810. (d) Tsuie, B.; Swenson, D. C.; Jordan, R. J.; Petersen, J. L. *Organometallics* **1997**, *16*, 1392. (e) Baumann, R.; Davis, W. M.; Schrock, R. R. *J. Am. Chem. Soc.* **1997**, *119*, 3830. (f) Gibson, V. C.; Kimberley, B. S.; White, A. J. P.; Williams, D. J.; Howard, P. *Chem. Commun.* **1998**, 313.

(5) (a) Giannini, L.; Solari, E.; Floriani, C.; Chiesi-Villa, A.; Rizzoli, C. *Angew. Chem., Int. Ed. Engl.* **1994**, *33*, 2204. (b) Uhrhammer, R.; Black, D. G.; Gardner, T. G.; Olsen, J. D.; Jordan, R. F. *J. Am. Chem. Soc.* **1993**, *115*, 8493, and references therein.

(6) (a) Solari, E.; Musso, F.; Floriani, C.; Chiesi-Villa, A.; Rizzoli, C. *J. Chem. Soc., Dalton Trans.* **1994**, 2015. (b) Brand, H.; Arnold, J. *Angew. Chem., Int. Ed. Engl.* **1994**, *33*, 95, and references therein.

(7) van der Linden, A.; Schaverien, C. J.; Meijboom, N.; Ganter, C.; Orpen, A. G. *J. Am. Chem. Soc.* **1995**, *117*, 3008.

(8) Hitchcock, P. B.; Lappert, M. F.; Liu, D.-S. *J. Chem. Soc., Chem. Commun.* **1994**, 2637.

10.1021/om980850b CCC: $18.00
Publication on Web 03/19/1999

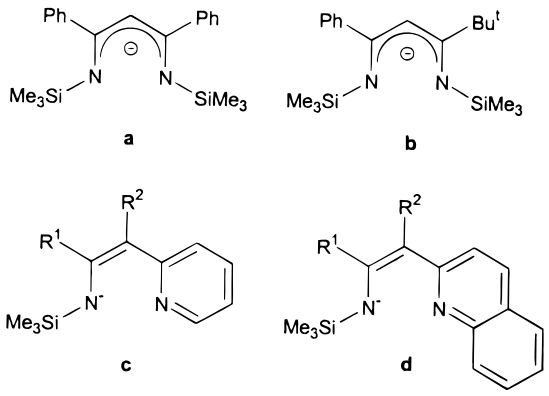

Figure 1. β-Diketiminato ligands **a** and **b** and the newly developed 2-pyridyl- (**c**) and 2-quinolyl- (**d**) substituted 1-azaallyl ligands.

β-diketiminate-based ligands that possess a nitrogen heterocycle (pyridine or quinoline) as part of the ligand backbone (**c** and **d** in Figure 1). These monoanionic *N*,*N*′-bidentate ligands, which were readily obtained as lithium derivatives from lithiated 2-methylpyridine or 2-methylquinoline by a 1,2 insertion of a suitable nitrile R^1CN (R^1 = Ph or Bu^t) into the Li−C bond followed by a 1,3 trimethylsilyl shift,[10] are less bulky than the above *N*,*N*′-bis(trimethylsilyl)-β-diketiminates (**a** and **b** in Figure 1) and were expected to have both good σ- and π-donating properties. Apart from being a variation on the β-diketiminate theme, we anticipated that, because of the less sterically demanding nature of the ligands, formation of bis(ligand)zirconium dichloride derivatives might be feasible, which would place the zirconium center into a chiral C_2 symmetrical coordination environment, forcing the chlorine atoms into *cis* positions.

In a preliminary communication we reported on some lithium and zirconium complexes of these pyridyl- and quinolyl-1-azaallyl ligands[11] and noted that the bis(ligand)zirconium(IV) chlorides with *cis* chloride ligands were indeed chiral, having either C_1 or C_2 symmetries. Details on the synthesis and characterization of the lithium complexes were reported in a previous paper.[10] Herein we provide full details on (i) the synthesis and characterization of the new zirconium(IV) and hafnium(IV) bis(1-azaallyl) chlorides and zirconium(IV) mono(1-azaallyl) chlorides and (ii) their catalytic activity in olefin polymerization when activated with MAO.

Results and Discussion

Preparation and Structural Characterization of the Complexes. Each of the lithium derivatives of the 2-pyridyl- and 2-quinolyl substituted 1-azaallyl ligands (**1a**−**5a**)[10] reacted smoothly with $ZrCl_4$ in Et_2O or THF to form racemic mixtures of bis(1-azaallyl)zirconium dichlorides **1b**−**5b** (Scheme 1). According to their NMR spectral data (Tables 1 and 2), these bis(1-azaallyl)-zirconium dichlorides adopt C_2 symmetrical geometries except for **4b**, which has no symmetry element (C_1). For

Scheme 1

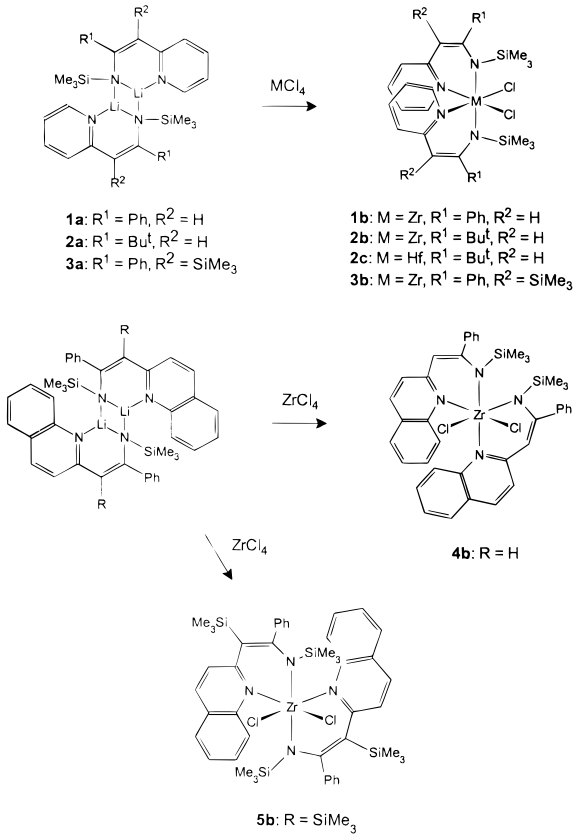

the highly substituted derivative **3b**, two sets of ^{1}H resonances for the *ortho*-protons of the phenyl groups (δ = 7.68 and 7.63, intensity ratio = 1:1) and two ^{13}C signals for the *C*SiMe$_3$ fragment (δ = 118.6 and 118.3) were observed, which is attributed to different puckering modes of the highly substituted ZrNCCCN metallacycles and hindered rotation of the phenyl group (vide infra). It should be noted that no other isomers were observed according to the NMR spectra of each of the purified complexes **1b**−**5b**. The hafnium congener of **2b**, i.e., **2c**, was prepared similarly from **2a** and $HfCl_4$. The elemental analytical data for **1b**, **2b**, and **5b** were poor, believed to be due to occluded LiCl.

The molecular structures of each of the crystalline complexes **2b**, **2c**, and **3b** were established by X-ray crystallography and are illustrated in Figures 2, 3, and 4, respectively; selected structural parameters for **2b** and **2c** are listed in Table 3. A detailed discussion of the molecular structure of complex **3b** has already been communicated.[11] Important structural features of all three compounds are (i) the distorted octahedral coordination geometry about the metal center and (ii) the *cis*-disposition of the chloride ligands. This *cis*-arrangement is also observed in zirconocene dichlorides and is crucial from a catalytic standpoint. In complex **2b** the 2-pyridylazaallyl ligand is coordinated in a η^1,η^3-fashion with a η^3-bonded azaallyl part of the ligand supplemented by a σ-bonded pyridyl moiety. For the isoleptic hafnium complex **2c** it was found that, although the overall structure is rather similar, the long M−C distances (all above 2.9 Å) indicate that the η^3-interaction is no longer present, which may well be the result of smaller covalent contributions in the ligand-to-metal bonding for hafnium. The "wrapping" of the ligand

(9) Lappert, M. F.; Liu, D.-S. Neth. Pat. Appl. 9500085, 1995.
(10) Deelman, B.-J.; Lappert, M. F.; Lee H.-K.; Mak, T. C. W.; Leung, W.-P.; Wei, P.-R. *Organometallics* **1997**, *16*, 1247.
(11) (a) Deelman, B.-J.; Hitchcock, P. B.; Lappert, M. F.; Lee, H.-K.; Leung, W.-P. *J. Organomet. Chem.* **1996**, *513*, 281. (b) Kristen, M. O.; Görtz, H. H.; Deelman, B. J.; Lappert, M. F.; Lee, H.-K.; Leung, W. P. Germ. Pat. Appl. 97105878.9-2109, 1997.

Table 1. ^{1}H NMR Data

compound	aryl	CH	Bu^t	SiMe$_3$
1b[a,c]	9.04 (d, J = 6.0 Hz, 2H, 6-py)	6.05		0.21
	7.66 (d, J = 7.2 Hz, 4H, *o*-Ph)			
	7.1−7.0 (m, 6H, *m*-Ph, *p*-Ph)			
	6.77 (t, J = 7.7 Hz, 2H, 4-py)			
	6.35 (d, J = 7.9 Hz, 2H, 3-py)			
	6.30 (t, J = 6.6 Hz, 2H, 5-py)			
2b[b,c]	10.18−10.16 (d, 1H, 6-py)	5.81	0.79	0.43
	6.98−6.92 (dt, 1H, 3-py)			
	6.57−6.49 (m, 2H, 4,5-py)			
2c[b,c]	10.14−10.12 (d, 1H, 6-py)	5.74	0.76	0.39
	6.92−6.85 (d, 1H, 3-py)			
	6.49−6.44 (m, 2H, 4,5-py)			
2d[b,c]	10.48 (m, 1H, 6-py)	5.21	1.13	0.24
	8.30−8.28 (d, 1H, 3-py)			
	6.52−6.47 (m, 2H, 4,5-py)			
3b[a,c]	8.58 (d, J = 4.7 Hz, 2H, 6-py)			0.03
	7.69 (d, J = 5.3 Hz, 2H, *o*-Ph)			0.01
	7.63 (d, J = 6.8 Hz, 2H, *o*-Ph)			
	7.28 (d, J = 8.0 Hz, 2H, 3-py)			
	7.12 (m, 6H, *m*-Ph, *p*-Ph)			
	6.87 (t, J = 6.9 Hz, 2H, 4-py)			
	6.00 (t, J = 6.8 Hz, 2H, 5-py)			
3d[b,e]	8.88 (d, J = 5.4 Hz, 1H, py)			−0.09
	8.36 (t, J = 8.1 Hz, 1H, py)			−0.28
	7.79 (d, J = 8.1 Hz, 1H)			
	7.73−7.42 (6H, Ph and py)			
4b[b,c]	9.30 (d br, J = 8.3 Hz, 1H, 9-qui)	5.63		0.36
	9.04 (m br, 1H, 9-qui)	5.48		0.18
	8.21 (s br, 2H, qui)			
	7.69 (d br, J = 5.1 Hz, 2H, *o*-Ph)			
	7.31−6.82 (14H, *p*-Ph, *m*-Ph, qui)			
	6.20 (d, J = 8.6 Hz, 1H, qui)			
	5.65 (d, J = 8.7 Hz, 1H, qui)			
5b[a,c]	8.82 (d, J = 8.3 Hz, 2H, 9-qui)			0.09
	8.28 (d, J = 8.4 Hz, 2H, qui)			0.08
	7.80 (d, J = 6.9 Hz, 2H, *o*-Ph)			
	7.54 (d, J = 8.6 Hz, 2H, *o*-Ph)			
	7.26−7.17 (m, 8H, *p*-Ph, *m*-Ph, qui)			
	6.77−6.75 (m, 2H, qui)			
	6.60−6.57 (m, 4H, qui)			
5d[a,e]	8.80 (d, J = 8.7 Hz, 1H, qui)			0.26
	8.75 (d, J = 8.4 Hz, 1H, qui)			−0.10
	8.0−7.5 (14H, Ph and qui)			−0.20
	7.40 (t, J = 7.5 Hz, 1H)			−0.31
	7.25 (t, J = 7.7 Hz, 1H)			
	6.95 (t, J = 7.3 Hz, 1H)			
	6.86 (t, J = 7.6 Hz, 1H)			
	6.65 (d, J = 8.4 Hz, 1H, qui)			
	6.34 (d, J = 8.6 Hz, 1H, qui)			

[a] 360 MHz. [b] 250 MHz. [c] In benzene-d_6. [d] In THF-d_8. [e] In dichloromethane-d_2.

around the metal center in **2b** and **2c** is markedly different from the η^2-bonding mode observed in the solid-state structure of **3b** (Figure 5). This is most probably caused by the higher degree of substitution of the 3-(2-pyridyl)-1-azaallyl, preventing π-coordination of the azaallyl part of the ligand system. A comparison of selected structural parameters for the three complexes is presented in Table 4.

The above results indicate that the 2-pyridylazaallyl ligand can adopt different bonding modes. Depending on the steric requirements of the substituents on the ligand backbone and the electronic requirements at the metal center, the ligand is able to behave as either an η^2- or η^1,η^3-donor.

Complexes **2b**, **2c**, and **3b** are structurally similar to (i) the Schiff-base complexes $[ZrL_2Cl_2]$ (L = a norephedrine-derived ligand, Cl−Zr−Cl = 93.7(1)°),[20] (ii) $[Zr(msal)_2Cl_2]$ (msal = *N*-methylsalicylideneiminate, Cl−Zr−Cl = 96.9(1)° and 98.8(1)°),[2b] and (iii) the benzamidinates $[M\{N(SiMe_3)C(Ph)N(SiMe_3)\}_2Cl_2]$ (M = Ti, Zr; Cl−Ti−Cl = 98.6(1)°, Cl−Zr−Cl = 103.8(1)°),[3a,d] which also have their chloride ligands *cis*-dispositioned in distorted octahedral metal coordination environments.

The mono(1-azaallyl)zirconium(IV) trichlorides **2d**, **3d**, and **5d** were readily obtained by conproportionation of complex **2b**, **3b**, or **5b** with $ZrCl_4$ in either dichloromethane or toluene as solvent (eq 1). All three compounds gave satisfactory NMR spectral data (Tables 1 and 2) and for **3d** and **5d** MS and elemental analyses data. It is noteworthy that **5d** showed two sets of ligand resonances in both the ^{1}H and ^{13}C NMR spectra, indicating that this compound is probably dimeric in solution. It is likely that compounds **2d** and **3d** are also dinuclear, but this is not firmly established. Mass spectra show that compounds **3d** and **5d** easily form monomeric molecular ions in the gas phase under EI conditions.

$$[Zr(LL)_2Cl_2] + ZrCl_4 \longrightarrow 2\,Zr(LL)Cl_3 \quad (1)$$

2d, **3d**, **5d**

2d: LL = [(N(SiMe$_3$)C(Bu^t)C(H)(C$_5$H$_4$N-2)]
3d: LL = [(N(SiMe$_3$)C(Ph)C(SiMe$_3$)(C$_5$H$_4$N-2)]
5d: LL = [(N(SiMe$_3$)C(Ph)C(SiMe$_3$)(C$_9$H$_6$N-2)]

Molecular Orbital Description of the Bis(pyridyl-1-azaallyl)zirconium Fragments. To investigate the electronic properties of the bis(pyridyl-1-azaallyl) group 4 metal complexes and to compare them to the well-known bis(cyclopentadienyl)metal complexes, we performed simple EHMO calculations on the idealized C_2 symmetrical model systems $[Zr(LL)_2]^{2+}$ (LL = {N(H)C(H)C(H)(C$_5$H$_4$N-2)}). To compare the effect of the differing coordination modes of the pyridyl-1-azaallyl ligand in **2b** and **3b**, both geometries were considered in the calculations, i.e., structures **A** and **B**, respectively (Figure 6). Throughout this discussion the labeling scheme of Figure 5 is adopted.

From ligand-to-metal overlap populations it is concluded that the bis(pyridylazaallyl) ligand environment is more electron-donating than that of bis(cyclopentadienyl) (Table 5). Hence, the metal center in the bis(pyridyl-1-azaallyl)metal complexes is less electrophilic than in the corresponding bis(cyclopentadienyl) systems. The interaction of the pyridyl-1-azaallyl ligand with the metal center in **A** (overlap population = 1.73) is slightly stronger than that for **B** (overlap population = 1.67), which corresponds to the higher substituted and less flexible ligand system of complex **3b**. This is not due to weaker Zr−N overlap populations in **B**, since in **B** the Zr−N(amide) interactions are markedly stronger due to the π-N→Zr overlap with the Zr d_{yz} orbital (overlap population 0.10). Such a π-contribution is almost absent in **A** (overlap population 0.02). However, in **A** there are stabilizing interactions with the carbon atoms C2 (overlap population 0.03) and C3 (overlap population 0.09) of the 1-azaallyl ligand. In **B**, interaction of the metal center with these atoms is destabilizing, resulting in a less favorable interaction. In conclusion, the higher steric congestion in **3b** than **2b** results in a weaker interaction of the pyridyl-1-azaallyl ligand with the metal center for **3b**.

The empty frontier orbitals of **A** and **B** that can participate in bonding of two additional σ-donating

Table 2. ^{13}C NMR Data

compound	aryl	CH or *C*SiMe$_3$	NCPh or NCBu^t	C*Me*$_3$	SiMe$_3$
1b[a,d]	154.2, 149.8, 141.2, 138.0, 129.2, 128.8, 127.9, 123.3, 120.2	111.2	155.0		3.1
2b[a,d]	156.4, 151.4, 138.1, 123.7, 120.9	111.5	170.6	38.2 30.5	4.0
2c[a,d]	157.1, 151.2, 138.0, 123.9, 120.5	112.3	171.1	38.5 30.8	4.3
2d[a,d]	150.1, 147.3, 135.3, 122.0, 116.3	89.9	161.4	35.8 29.2	1.3
3b[a,d]	162.9, 149.8, 143.4, 137.9, 134.4, 130.4, 129.3, 128.6, 128.4, 128.3, 127.9, 127.0, 125.8	118.6, 118.3	165.0		4.3, 2.3
3d[b,f]	151.8, 148.3, 143.0, 142.1, 131.0, 130.7, 129.5, 129.1, 128.9, 127.2, 126.9	123.2	160.0		1.83 0.95
4b[a,g]	155.2, 152.5, 145.8, 145.4, 142.3, 138.4, 138.2, 138.1, 137.3, 130.8, 130.5, 130.2, 127.0, 126.9, 126.9, 126.4, 125.3, 124.9, 121.9, 120.4	105.3, 91.4	165.1		4.3 3.7
5b[a,c]	163.5, 145.8, 142.8, 138.7, 135.1, 131.5, 130.7, 129.8, 127.3, 126.9, 126.5, 125.3, 124.9, 119.5, 118.4	104.9	166.5		3.9 2.6
5d[b,f,h]	161.9, 145.2, 144.1, 144.0, 142.6, 141.9, 140.5, 133.1, 132.0, 131.6, 131.2, 130.9, 129.7, 129.3, 129.0, 128.9, 128.5, 127.2, 126.5, 125.0, 124.0, 123.8, 123.3	112.9	163.6		3.3 3.0 2.8 0.2

[a] 62.9 MHz. [b] 75.5 MHz. [c] Benzene/benzene-d_6. [d] Benzene-d_6. [e] THF-d_8. [f] Dichloromethane-d_2. [g] Toluene/toluene-d_8. [h] Low signal/noise ratio due to low solubility.

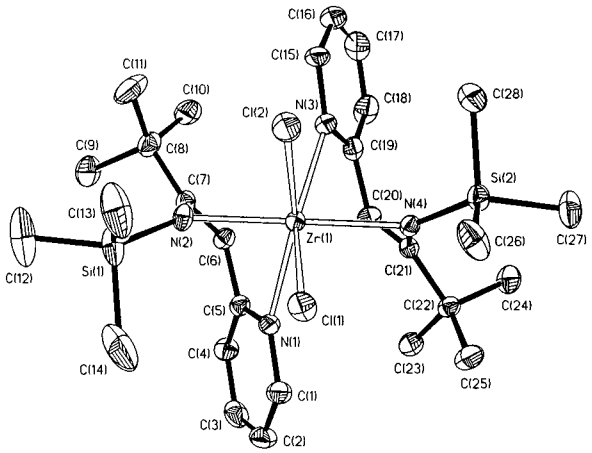

Figure 2. Molecular structure of [Zr{N(SiMe$_3$)C(Bu^t)C(H)(C$_5$H$_4$N-2)}$_2$Cl$_2$] (**2b**) showing atom-labeling scheme. The thermal ellipsoids are drawn at the 20% probability level.

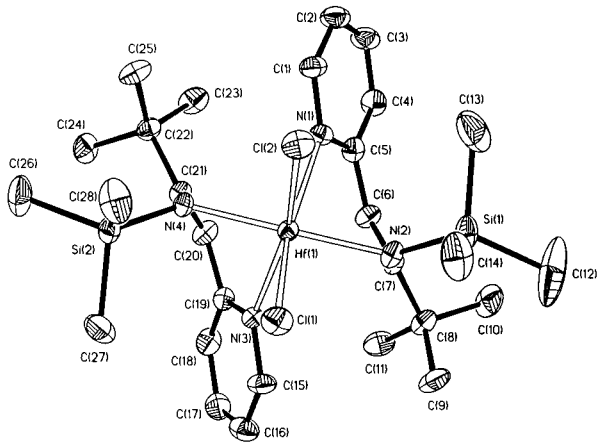

Figure 3. Molecular structure of [Hf{N(SiMe$_3$)C(Bu^t)C(H)(C$_5$H$_4$N-2)}$_2$Cl$_2$] (**2c**) showing atom-labeling scheme. The thermal ellipsoids are drawn at the 20% probability level.

ligands (e.g., H$^-$, Cl$^-$, or alkyl$^-$) are represented in Figure 6 along with those of [Zr(η^5-C$_5$H$_5$)$_2$]$^{2+}$ (**C**) for comparison.[12] It should be noted that these relevant frontier orbitals are similar in symmetry and shape for all three fragments **A**, **B**, and **C**. However, due to the strong σ-donation of the pyridyl groups to the d_{xz} orbital of zirconium, molecular orbital 24b of fragment **A** is substantially raised in energy compared to the corresponding orbital (6b2) of the biscyclopentadienylzirconium fragment **C**. For **B** this effect is even more pronounced, and in addition the acceptor orbital of "a" symmetry (27a) is also significantly raised in energy.

To probe the bonding of additional σ-donors, hypothetical dihydrides [Zr(LL)$_2$H$_2$] were constructed for both ligand arrangements. From Zr−H overlap populations it follows that, despite the fact that the metal acceptor orbitals for [Zr(LL)$_2$]$^{2+}$ are at higher energy than in **C**, this does not significantly affect the Zr−H bond (Table 5). Mixing-in of lower lying filled orbitals is responsible for this effect. Hence, in comparing different metal−ligand combinations, shape and symmetry of the fragment frontier orbitals are more informative than the exact energies of those orbitals. For a better comparison, the actual overlap populations with additional ligands entering the metal coordinaton sphere should be considered.

Olefin Polymerization Activity of the Complexes. Each of the bis(1-azaallyl)zirconium(IV) chlorides **1b**−**5b**, combined with a large excess of MAO, was tested for catalytic activity in ethylene polymerization. However, only complex **2b** was found to display modest activity.[13] In contrast, mono(1-azaallyl)zirconium(IV)

(12) Lauher, J. W.; Hoffmann, R. *J. Am. Chem. Soc.* **1976**, *98*, 1729.

(13) 1.4 kg of PE mol^{-1} Zr h^{-1} ([Zr] = 0.70 mM, Al/Zr = 200, T = 25 °C, p = 1 bar).

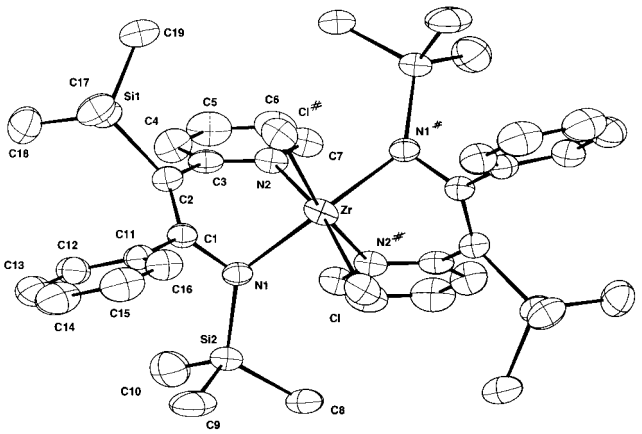

Figure 4. Molecular structure of [Zr{N(SiMe$_3$)C(Ph)C(SiMe$_3$)(C$_5$H$_4$N-2)}$_2$Cl$_2$] (**3b**) showing atom-labeling scheme. The thermal ellipsoids are drawn at the 50% probability level.

Table 3. Selected Bond Distances (Å) and Angles (deg) for [M{N(SiMe$_3$)C(Bu^t)C(H)(C$_5$H$_4$N-2)}$_2$Cl$_2$] (M = Zr (2b); M = Hf (2c))

2b		2c	
Zr(1)−Cl(1)	2.5015(12)	Hf(1)−Cl(1)	2.429(1)
Zr(1)−Cl(2)	2.5252(12)	Hf(1)−Cl(2)	2.419(1)
Zr(1)−N(1)	2.322(3)	Hf(1)−N(1)	2.335(1)
Zr(1)−N(2)	2.191(3)	Hf(1)−N(2)	2.142(1)
Zr(1)−N(3)	2.311(3)	Hf(1)−N(3)	2.326(1)
Zr(1)−N(4)	2.231(3)	Hf(1)−N(4)	2.158(1)
Zr(1)−C(6)	2.756(4)	Hf(1)−C(6)	3.172(2)
Zr(1)−C(7)	2.655(4)	Hf(1)−C(7)	2.909(2)
Zr(1)−C(20)	2.708(4)	Hf(1)−C(20)	3.199(2)
Zr(1)−C(21)	2.678(4)	Hf(1)−C(21)	2.922(2)
N(1)−C(5)	1.349(5)	N(1)−C(5)	1.325(1)
N(2)−C(7)	1.359(5)	N(2)−C(7)	1.397(1)
N(3)−C(19)	1.337(5)	N(3)−C(19)	1.343(2)
N(4)−C(21)	1.357(5)	N(4)−C(21)	1.391(2)
C(5)−C(6)	1.439(5)	C(5)−C(6)	1.461(1)
C(6)−C(7)	1.396(5)	C(6)−C(7)	1.353(2)
C(19)−C(20)	1.457(5)	C(19)−C(20)	1.455(1)
C(20)−C(21)	1.384(5)	C(20)−C(21)	1.326(1)
Cl(1)−Zr−Cl(2)	81.38(4)	Cl(1)−Hf−Cl(2)	83.4(1)
N(1)−Zr−N(3)	128.57(11)	N(1)−Hf−N(3)	115.0(1)
N(2)−Zr−N(4)	178.14(12)	N(2)−Hf−N(4)	157.5(1)

chlorides **2d**, **3d**, and **5d** displayed activities in the range 6−75 kg of PE mol^{-1} Zr h^{-1} with the activity order **5d** < **3d** < **2d** ([Zr] = 1.5 mM, Al/Zr = 100, T = 25 °C, p = 1 bar). Under these conditions, **3d** (20 kg mol^{-1} Zr h^{-1}) showed activity similar to [Zr(η^5-C$_5$H$_5$)$_2$Cl$_2$]/MAO (38 kg mol^{-1} Zr h^{-1}), which is known to be one of the most active systems in ethylene polymerization.[1b] The activities found should be regarded as lower limits to the intrinsic activity of these complexes since we did not make attempts to optimize [Zr] and Al/Zr ratios. Also for the most active catalysts (**2d** and [Cp$_2$ZrCl$_2$]) mass transport limitation cannot be excluded. Although GPC analysis of the PE produced was hindered by the extremely low solubility of the polymer samples in 1,2-dichlorobenzene even at high temperature, intrinsic viscosity ([η]) measurements were indicative of high molecular weight.[14]

Complex **3d** was tested in the polymerization of propylene and styrene but was found to be inactive under ambient conditions. For 1-hexene some oligomerization (0.133 g mol^{-1} Zr h^{-1}) was observed, which is probably a concentration effect.[15] End-group analysis of the oligohexenes formed (^{1}H NMR) indicated that the material consisted of substantial amounts (68%) of oligomers terminated by internal double bonds (δ = 5.37−5.34); the signals observed at δ = 133.4−125.3 in the ^{13}C NMR spectrum are also typical for internal double bonds.[7] In addition, vinylidene (H$_2$C=C(R)R′, 27%) and allyl (H$_2$C=CHCH$_2$R, 5%) terminated oligo-

(14) Intrinsic viscosity values ([η]) of 9.1 (**3d**) and 7.3 dL/g (**5d**) were measured.

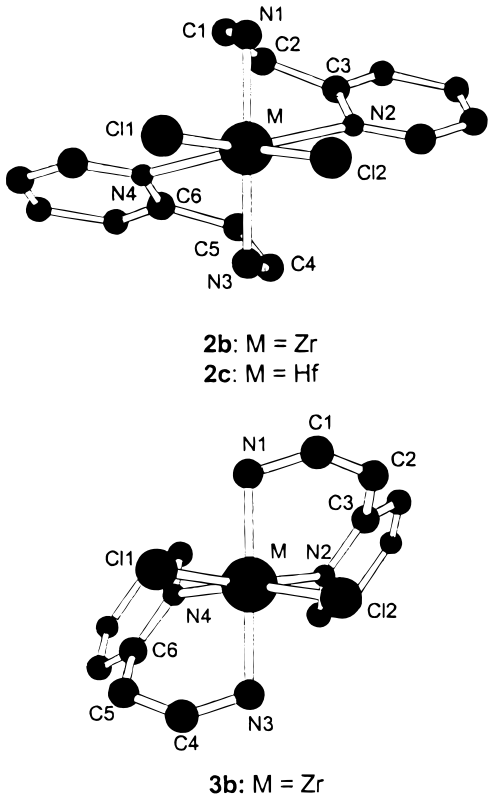

Figure 5. Comparison of the two bonding modes of the 3-(2-pyridyl)-1-azaallyl ligands in [M{N(SiMe$_3$)C(R^1)C(R^2)(C$_5$H$_4$N-2)}$_2$Cl$_2$] complexes (M = Zr, R^1 = Bu^t, R^2 = H (**2b**); M = Hf, R^1 = Bu^t, R^2 = H (**2c**); R^1 = Ph, R^2 = SiMe$_3$ (**3b**)). Hydrogen atoms and ligand substituents have been omitted for clarity. For better comparison the structural drawing corresponding to **2b** and **2c** (top) is drawn in its opposite enantiomeric representation.

Table 4. Comparison of Selected Bond Distances and Angles in Complexes 2b, 2c, and 3b According to Labeling Scheme of Figure 5

bond distance (Å) or angle (deg)	**2b** (M = Zr)	**2c** (M = Hf)	**3b** (M = Zr)
M−Cl(1)	2.5252(12)	2.429(1)	2.434(1)
M−Cl(2)	2.5015(12)	2.419(1)	2.434(1)
M−N(1)	2.191(3)	2.142(1)	2.141(3)
M−N(2)	2.322(3)	2.335(1)	2.354(3)
M−N(3)	2.231(3)	2.158(1)	2.141(3)
M−N(4)	2.311(3)	2.326(1)	2.354(3)
M−C(1)	2.655(4)	2.909(2)	2.868(4)
M−C(2)	2.756(4)	3.172(2)	3.277(4)
M−C(4)	2.678(4)	2.922(2)	2.868(4)
M−C(5)	2.708(4)	3.199(2)	3.277(4)
Cl(1)−M−Cl(2)	81.38(4)	83.4(1)	95.06(7)
N(1)−M−N(3)	178.14(12)	157.5(1)	165.0(2)
N(2)−M−N(4)	128.57(11)	115.0(1)	76.7(2)

(15) The solubility of propene in toluene under the conditions employed is only 0.9 M (Plöcker, U.; Knapp, H.; Prausnitz, J. *Ind. Eng. Chem. Process Des. Rev.* **1978**, *17* (3), 324), whereas the concentration of 1-hexene was 5.1 M.

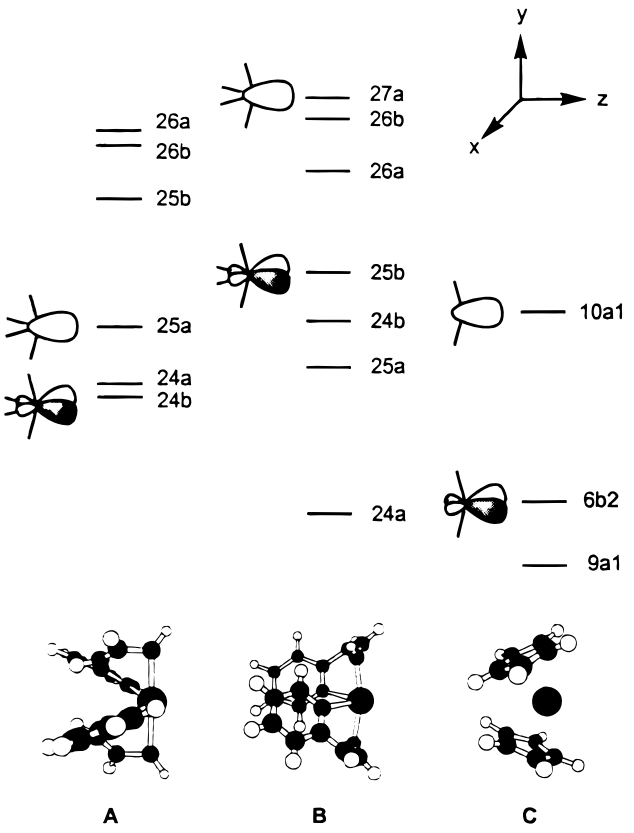

Figure 6. Energy level diagram of frontier acceptor orbitals of $[Zr(LL)_2]^{2+}$ and $[Zr(\eta^5\text{-}C_5H_5)_2]^{2+}$ fragments.

Table 5. Overlap Populations Calculated for Model Fragments $[Zr(LL)_2]^{2+}$ (LL = N(H)C(H)C(H)(C_5H_4N-2)) and $[ZrCp_2]^{2+}$ (Cp = η^5-C_5H_5)

overlap population	$[Zr(LL)_2]^{2+}$ (A)	$[Zr(LL)_2]^{2+}$ (B)	$[ZrCp_2]^{2+}$
Zr−{(LL)$_2$} or Zr−{Cp$_2$}	1.73	1.67	1.42
Zr−{N(amido)}	0.49	0.59	
Zr−{N(py)}	0.41	0.43	
Zr−H (in $Zr(LL)_2H_2$ or $Zr(Cp)_2H_2$)	0.61	0.62	0.62

mers were observed (^{1}H NMR: δ = 5.80 (m, 1H, CH_2=C(*H*)CH_2R), 5.01−4.90 (m, 2H, C*H*$_2$=C(H)CH_2R) and 4.72−4.56 (4 × s, C*H*$_2$=C(R)R′)).[17] A value of M_n = 950 was deduced from the relative intensities of end-group signals and aliphatic hydrogen signals.

Complex **3d** was also found to be active in copolymerization of ethylene and 1-hexene (2.7 kg of polymer mol^{-1} Zr h^{-1}). End-group analysis of the toluene-soluble fraction again indicated the presence of internal double bonds (59%), vinylidene groups (26%), and allyl groups (15%). From relative intensities of the methyl region and the methylene/methine region of the ^{1}H NMR spectrum, the ratio of 1-hexene to ethylene units in the toluene-soluble fraction of the copolymer was calculated to be ca. 1.5. Relative intensities of the aliphatic region and the end-group resonances indicated that M_n = 1900.

Vinylidene end-groups in the copolymer are attributed to a primary 1,2-insertion of 1-hexene followed by β-H elimination, whereas allylic end-groups most probably originate from final ethylene insertions followed by β-H elimination. However, the presence of RCH=CHR′ end-groups in both the oligohexenes and the 1-hexene/ethylene copolymer implies that a favorable termination pathway involves secondary 2,1-insertion of 1-hexene followed by β-hydrogen elimination. Brintzinger et al.[16] have shown that for metallocene/MAO systems these 2,1-misinsertions result in the formation of dormant sites for which further insertion of monomer is sterically substantially hindered. The formation of dormant sites resulting from 2,1-insertion of olefin could also account for the inactivity of **3d** in propene polymerization and the low activity of **3d** in 1-hexene polymerization. Another noteworthy observation is the presence of allyl end-groups in the oligohexenes, possibly due to chain termination by β-alkyl elimination.[17]

The low activity of the bis(1-azaallyl) complexes in ethylene polymerization cannot be explained a priori by pure steric considerations. Molecular mechanics studies indicated that there is enough space for a coordinating alkyl chain (R$^-$) and an ethylene molecule to occupy *cis*-positions in the coordination gap of a $[Zr(LL)_2]^{2+}$ fragment (LL = 3-(2-pyridyl)-1-azaallyl ligand). The resulting hypothetical $[Zr(LL)_2(R)(CH_2CH_2)]^+$ species would be the 1-azaallyl analogue of the presumed active species in metallocene-based Ziegler−Natta polymerization, i.e., $[Zr(\eta^5\text{-}C_5H_5)_2(R)(CH_2CH_2)]^+$.[1]

One feasible explanation for the inactivity of the bis-(1-azaallyl)zirconium complexes in ethylene polymerization might be that the $[Zr(LL)_2]^{2+}$ fragment, unlike its cyclopentadienyl counterpart, possesses empty low lying pyridyl (or quinolyl) π* levels, which renders the 1-azaallyl ligands susceptible to nucleophilic attack by incoming alkyl nucleophiles. This hypothesis is supported by the reaction of **5b** with $PhCH_2MgCl$ (2 equiv in Et_2O), which resulted in nucleophilic attack by the benzyl group at the 4-position of the quinoline functionality to form **5e** (eq 2). The ^{1}H NMR spectrum of this compound displayed a typical ABX pattern for the C(*H*)-(C*H*$_2$Ph) moiety and a doublet (δ = 4.84) which was assigned to the NC=C(*H*)−CH fragment. The ^{13}C NMR spectrum displayed a characteristic *C*(H)(CH_2Ph) resonance (δ = 49.4). Consequently, it seems feasible that alkylation by a large excess of MAO, which can also contain substantial amounts of $AlMe_3$, could lead to nucleophilic attack on one (or both) of the 1-azaallyl ligands, producing an inactive complex.

Although we have not investigated this option in detail we do not think that ligand transfer to aluminum could explain the low activity of the bis(pyridyl-1-azaallyl)zirconium complexes since such a process would, at least in the first step, lead to formation of mono-(pyridyl-1-azallyl)zirconium species which are expected to be very similar in nature to the species resulting from reaction of the mono(pyridyl-1-azaallyl)zirconium trichlorides with MAO. However, for the mono(pyridyl-1-azaallyl)zirconium trichlorides themselves such a process remains a feasible option. Since our primary interest in these group 4 metal complexes was to investigate whether they could serve as catalysts for stereoregular polymerization of propene and higher 1-alkenes, we did not investigate this aspect any further once it had

(16) (a) Stehling, U.; Diebold, J.; Kirsten, R., Röll, W.; Brintzinger, H.-H.; Jüngling, S.; Mülhaupt, R.; Langhauser, F. *Organometallics* **1994**, *13*, 964. (b) Jüngling, S.; Mülhaupt, R.; Stehling, U.; Brintzinger, H.-H.; Fischer, D.; Langhauser, F. *Macromol. Symp.* **1995**, *97*, 205.

(17) Resconi, L.; Piemontesi, F.; Franciscono, G.; Abis, L.; Fiorani, T. *J. Am. Chem. Soc.* **1992**, *114*, 1025.

become clear to us that none of the complexes prepared displayed the desired property.

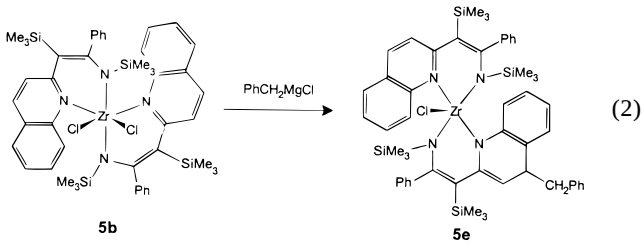

(2)

Conclusions

We have shown that the newly developed pyridyl- and quinolyl-susbtituted 1-azaallyl ligands can be successfully introduced on group 4 metals, stabilizing these highly electrophilic metal centers and providing an easy access to racemic mixtures of nonsymmetrical and C_2 symmetrical complexes. The absence of *meso* forms is a major synthetic advantage when compared to the synthesis of chiral *ansa*-metallocene derivatives. The 1-azaallyl ligands are highly electron-donating, and the metal frontier orbitals of bis(1-azaallyl)M species are comparable in shape to those of the M(η^5-C_5H_5)$_2$ fragment of bent metallocenes. Sterically these novel ligands are very demanding and perhaps even more so than bulky cyclopentadienyls.

Despite the electronic analogy between them, the bis(1-azaallyl)zirconium dichloride complexes are inactive in ethylene polymerization, whereas zirconocene dichlorides belong to the most active precatalysts known to date. One feasible explanation for this inactivity is nucleophilic alkylation of the 1-azaallyl ligands. Mono(1-azaallyl)zirconium trichlorides on the other hand were found to be highly active precatalysts with activities of the same order of magnitude as observed for [Zr(η^5-C_5H_5)$_2$Cl$_2$]. Activity is mainly limited to ethylene however. Although modest activity in copolymerization of ethylene with 1-hexene was observed, homopolymerization of higher olefins was much slower (1-hexene) or not taking place at all (propylene and styrene). For propene and 1-hexene this is presumably due to facile formation of dormant sites by 2,1-misinsertions, which is most likely the result of the open coordination sphere of the zirconium center in the catalytically active species.

Experimental Section

General Considerations. All experiments were performed under argon using standard Schlenk and vacuum line techniques. Pentane, Et_2O, THF, THF-d_8, cyclohexane, benzene, benzene-d_6, toluene, and toluene-d_8 were distilled from Na/K alloy and degassed prior to use. Polymerization grade ethylene and propylene (BOC) were purified by passing through BASF Cu catalyst and molecular sieves (4 Å) columns. MAO was obtained from Witco as a 10 wt % solution in toluene (density ≈ 0.9 g/mL). Other compounds were purchased and purified by standard procedures. NMR spectra were recorded on Bruker WM250, WM300, and WM360 spectrometers at ambient temperatures. MS spectra (EI) were recorded on a VG Autospec intrument. Elemental analyses were carried out by Medac Ltd. (Brunel University). Viscosity measurements were performed at BASF, Ludwigshaven. Molecular mechanics calculations were performed using the Hyperchem software package[18] with the standard MM+ parameter set.

[Zr{N(SiMe$_3$)C(Ph)C(H)(C$_5$H$_4$N-2)}$_2$Cl$_2$] (1b). A solution of **1a** (2.38, 4.34 mmol) in THF (12 mL) was added to a solution of $ZrCl_4$ (0.99 g, 4.25 mmol) in THF (60 mL) at 0 °C. The reaction mixture was allowed to reach room temperature, stirred for 15 h, and finally refluxed during 1.5 h, resulting in an orange-red solution. Volatiles were removed in a vacuum, and the residue was stripped with hexane (10 mL) and extracted with Et_2O (50 mL) and CH_2Cl_2 (2 × 10 mL). The combined extracts were concentrated to ca. 50 mL, and cooling to −30 °C afforded yellow crystals, which were washed with hexane (5 mL). Yield: 1.58 g (2.27 mmol, 53%). Anal. Calcd for $C_{32}H_{38}N_4Cl_2Si_2Zr$: C, 55.1; H, 5.50; N, 8.04. Found: C, 53.1; H, 5.42; N, 7.42. MS (EI, 70 eV): *m*/*z* 695 (31, $(M-1)^+$), 681 (9, $(M-Me)^+$), 659 (9, $(M-Cl)^+$), 623 (6, $(M-2Cl)^+$).

[Zr{N(SiMe$_3$)C(Bu^t)C(H)(C$_5$H$_4$N-2)}$_2$Cl$_2$] (2b). A solution of **1b** (1.74 g, 3.42 mmol) in Et_2O (40 mL) was added to a stirring suspension of $ZrCl_4$ (0.80 g, 3.43 mmol) in Et_2O (10 mL) at 0 °C. The yellow reaction mixture was allowed to reach room temperature and stirred for 20 h, and then volatiles were removed in a vacuum. The residue was extracted with toluene and filtered through Celite. Concentration to ca. 5 mL afforded bright yellow crystals of the product. Yield: 0.63 g (0.96 mmol, 28%). Anal. Calcd for $C_{28}H_{46}N_4Cl_2Si_2Zr$: C, 51.2; H, 7.06; N, 8.53. Found: C, 50.4; H, 6.93; N, 6.93.

[Hf{N(SiMe$_3$)C(Bu^t)C(H)(C$_5$H$_4$N-2)}$_2$Cl$_2$] (2c). A procedure similar to that used for **2b** was used, starting from $HfCl_4$ (0.38 g, 1.2 mmol). Yield: 0.44 g (0.59 mmol, 49%). Anal. Calcd for $C_{28}H_{46}N_4Cl_2Si_2Hf$: C, 45.2; H, 6.23; N, 7.53. Found: C, 45.1; H, 6.09; N, 6.97.

[Zr{N(SiMe$_3$)C(Ph)C(SiMe$_3$)(C$_5$H$_4$N-2)}$_2$Cl$_2$] (3b). Compound **3a** (3.86 g, 5.70 mmol) was added to $ZrCl_4$ (1.33 g, 5.71 mmol) in Et_2O (60 mL). The reaction mixture was stirred for 16 h, resulting in a yellow suspension. Volatiles were removed in a vacuum, and the residue was extracted with CH_2Cl_2 (2 × 50 mL) and filtered twice. Volatiles were removed from the filtrate in a vacuum, and crystallization from toluene (50 mL) at −30 °C afforded yellow crystals of **3b** (1.32 g, 1.57 mmol, 28%). Concentration of the mother liquor gave another 1.13 g. Total yield of **3b**: 2.45 g (3.1 mmol, 54%). Anal. Calcd for $C_{38}H_{54}Cl_2N_4Si_4Zr$: C, 54.2; H, 6.47; N, 6.66. Found: C, 54.2; H, 6.38; N, 6.56. MS (EI, 70 eV): *m*/*z* 840 (15, M^+), 825 (5, $(M-Me)^+$), 805 (11, $(M-Cl)^+$).

X-ray Structure Determinations of [M{N(SiMe$_3$)C(Bu^t)C(H)(C$_5$H$_4$N-2)}$_2$Cl$_2$] (M = Zr (2b); M = Hf (2c)) and [Zr{N(SiMe$_3$)C(Ph)C(SiMe$_3$)(C$_5$H$_4$N-2)}$_2$Cl$_2$] (3b). Selected single crystals of **2b**, **2c**, and **3b** were sealed in Lindemann glass capillaries under dinitrogen. For **2b** raw intensities were collected in the variable ω-scan mode on a four-circle diffractometer (Siemens P4 or Rigaku AFC7R) using Mo Kα radiation (λ = 0.710 73 Å) at 294 K. Determination of the crystal class and orientation matrix was performed according to established procedures. Unit-cell parameters were calculated from least-squares fitting of 2θ angles for 20 (or 25) selected reflections. Crystal stability was monitored by recording two (or three) check reflections at intervals of 100/150 data measurements, and no significant variation was detected. The raw data were processed with a learn-profile procedure,[19] and empirical absorption corrections were applied by fitting a pseusoellipsoid to the ψ-scan data of selected strong reflections over a range of 2θ angles. For **2c**, the intensity data were collected at 294 K on a MSC/Rigaku RAXIS-IIC imaging plate diffractometer using Mo Kα radiation (λ = 0.710 73 Å) from a Rigaku RU-200 rotating-anode generator operating at 50 kV and 90 mA ($2\theta_{min} = 2°$, $2\theta_{min} = 55°$ oscillation frames in the range 0−180°, exposure 8 min per frame). A self-consistent semiempirical absorption correction based on Fourier coefficient fitting of

(18) *HyperChem*, release 3 for Windows 3.1; Hypercube Inc.
(19) R. Diamond *Acta Crystallogr., Sect. A* **1968**, *25*, 43.

Table 6. Details of the X-ray Structure Determinations of [M{N(SiMe$_3$)C(R^1)C(R^2)(C$_5$H$_4$N-2)}$_2$Cl$_2$] (M = Zr, R^1 = Bu^t, R^2 = H (2b); M = Hf, R^1 = Bu^t, R^2 = H (2c); R^1 = Ph, R^2 = SiMe$_3$ (3b))

empirical formula	$C_{28}H_{46}Cl_2N_4Si_2Zr$ (**2b**)	$C_{28}H_{46}Cl_2N_4Si_2Hf$ (**2c**)	$C_{39}H_{56}Cl_4N_4Si_4Zr$ (**3b**)
fw	657	744.3	926.3
cryst size (mm)	0.20 × 0.20 × 0.70	0.12 × 0.22 × 0.24	0.50× 0.30× 0.25
cryst syst	orthorhombic	monoclinic	monoclinic
space group	*Pbca* (No. 61)	$P2_1/c$ (No. 14)	$P2/n$ (No. 13)
a (Å)	10.219(2)	21.407(4)	15.779(4)
b (Å)	15.543(3)	9.999(2)	9.331(4)
c (Å)	41.308(8)	15.823(3)	17.488(3)
α (deg)	90	90	90
β (deg)	90	104.17(3)	112.46(2)
γ (deg)	90	90	90
V (Å^3)	6561(3)	3283.8(2)	2379.5(13)
D_{calcd} (mg/m^3)	1.330	1.505	1.29
Z	8	4	2
F(000)	2752	1504	964
abs coeff (mm^{-1})	0.594	3.436	0.59
θ range for data collcn (deg)	2.58−27.5	2−55	2−25
index ranges	$0 \le h \le 13$, $0 \le k \le 20$, $0 \le l \le 53$	$-27 \le h \le 26$, $-11 \le k \le 11$, $0 \le l \le 19$	$0 \le h \le 18$, $0 \le k \le 11$, $-20 \le l \le 19$
no. of reflns collcd	7504	6787	4329
no. of indept reflns	7504	6526 [R(int) = 0.038]	4176 [R(int) = 0.0229]
no. of reflns with $I > 2\sigma(I)$	3636 [$I > 4\sigma(I)$]	5616 [$I > 8\sigma(I)$]	2914 [$I > 2\sigma(I)$]
structure solution	direct methods	direct methods	direct methods
refinement method	full-matrix least-squares on F^2	full-matrix least-squares on F^2	full-matrix least-squares on all F^2
no. of params refined	334	335	240
goodness-of fit	1.39	1.77	1.078 (on F^2)
final R indices (obs data)[a]	$R1 = 0.054$, $wR2 = 0.1315$	$R1 = 0.044$, $wR = 0.065$	$R1 = 0.050$, $wR2 = 0.123$
R indices (all data)	$R1 = 0.1511$, $wR2 = 0.1621$		$R1 = 0.081$, $wR2 = 0.140$
largest diff peak and hole, e A^{-3}	0.50, −0.43	1.1, −0.98	0.78, −0.50
abs corr from ψ scans	$T_{max} = 1.00$ $T_{min} = 0.985$		$T_{max} = 1.00$ $T_{min} = 0.96$
maximum shift/esd	0.002	0.002	0.002

[a] $R1 = \sum||F_0| - |F_c||/\sum|F_0|$, $wR = [\sum w(|F_0| - |F_c|)^2/\sum w|F_0|^2]^{-1}$, $wR2 = [\sum w(|F_0|^2 - |F_c|^2)^2/\sum w(|F_0|^2)^2]^{-1}$.

symmetry-equivalent reflections was applied by using the ABSCOR program.[20] The crystal structures of **2b** and **2c** were determined by the direct method, which yielded the positions of all non-hydrogen atoms, and all non-hydrogen atoms were subjected to anistropic refinement. The hydrogen atoms were generated geometrically (C−H bonds fixed at 0.96 Å and allowed to ride on their respective parent atoms); they were assigned appropriate isotropic temperature factors and included in the structure factor calculations. All computation were performed on an IBM-compatible PC with the Siemens SHELXTL PLUS program package.[21] Analytical expressions of neutral-atom scattering factors were employed, and anomalous dispersion corrections were incorporated. For **3b**, data were collected on an Enraf-Nonius CAD-4 diffractometer using monochromated Mo Kα (λ = 0.710 73 Å) radiation and corrected for Lorentz, polarization, and absorption effects. The structure was refined on F^2 using SHELXL-93.[22] Hydrogen atoms were included in riding mode. There is a molecule of CH_2Cl_2 solvate for which the C atom could not be located. Crystallographic data and further experimental details of the structure determinations for **2b**, **2c**, and **3b** are listed in Table 6.

[Zr{N(SiMe$_3$)C(Ph)C(H)(C$_9$H$_6$N-2)}$_2$Cl$_2$] (4b). To a stirred suspension of $ZrCl_4$ (1.15 g, 4.94 mmol) in Et_2O (100 mL) was added **4a** (3.13 g, 9.65 mmol), resulting in a yellow suspension. The reaction mixture was stirred for 15 h, and volatiles were removed in a vacuum. The residue was extracted with CH_2Cl_2 (1 × 30 mL, 1 × 10 mL). The filtrate was evaporated to dryness and suspended in hexane (20 mL). The solid was collected on a frit and washed with hexane (20 mL), affording a yellow powder (3.70 g). Recrystallization from CH_2Cl_2/hexane and hot toluene gave yellow needles of **4b** (2.76 g, 3.10 mmol, 65%). Anal. Calcd for $C_{40}H_{42}Cl_2N_4Si_2Zr(C_7H_8)$: C, 63.5; H, 5.67; N, 6.30. Found: C, 63.9; H, 5.67; N, 6.22. MS (EI, 70 eV): m/z 686 (26, $(M - SiMe_3Cl)^+$).

[Zr{N(SiMe$_3$)C(Ph)C(SiMe$_3$)(C$_9$H$_6$N-2)}$_2$Cl$_2$] (5b). To a stirred suspension of $ZrCl_4$ (0.50 g, 2.2 mmol) in Et_2O (50 mL) was added **5a** (1.70 g, 4.3 mmol), resulting in an orange suspension. The reaction mixture was stirred for 3 days, and volatiles were removed in a vacuum. The residue was extracted with warm toluene (45 mL). The filtrate was evaporated to dryness and the residue suspended in hexane (25 mL). The orange solid was collected and washed with hexane (20 mL). Recrystallization from CH_2Cl_2/Et_2O (1:1) afforded the orange microcrystalline solid **5b** (0.78 g, 0.83 mmol, 37%). Anal. Calcd for $C_{46}H_{58}Cl_2N_4Si_4Zr$: C, 58.7; H, 6.21; N, 5.95. Found: C, 56.8; H, 6.10; N, 4.84. MS (EI, 70 eV): m/z 834 (3, $((M - SiMe_3Cl)^+$). In another experiment starting from **5a** (12.7 g, 32.0 mmol), 8.14 g (8.65 mmol, 54%) of **5b** was obtained. Extraction was carried out with CH_2Cl_2 (200 mL) instead of toluene.

[Zr{N(SiMe$_3$)C(Bu^t)C(H)(C$_4$H$_5$N-2)}Cl$_3$] (2d). $ZrCl_4$ (0.11 g, 0.49 mmol) was added to a solution of **2b** (0.32 g, 0.49 mmol) in toluene (15 mL). After stirring for 10 h at 80 °C, volatiles were removed in a vacuum. Extraction with CH_2Cl_2, evaporation of the solvent from the extract, and washing with hot hexane (20 mL) afforded the orange solid **2d** (0.41 g, 95%).

[Zr{N(SiMe$_3$)C(Ph)C(SiMe$_3$)(C$_5$H$_4$N-2)}Cl$_3$] (3d). To a suspension of $ZrCl_4$ (0.63 g, 2.70 mmol) in toluene (35 mL) was added **3b** (2.16 g, 2.57 mmol). After stirring for 16 h a yellow oil had formed from which volatiles were removed in a vacuum. The residue was stripped and washed with hexane (20 mL), resulting in a yellow powder identified as **3d**. Yield: 1.73 g (3.22 mmol, 63%). MS (EI, 70 eV): m/z 536 (13, M^+), 521 (39, $(M - Me)^+$), 501 (45, $(M - Cl)^+$). Recrystallization from Et_2O/CH_2Cl_2 (1:1) afforded the mono ether adduct in essentially quantitative yield (^{1}H NMR). Anal. Calcd for $C_{23}H_{37}N_2Si_2ZrCl_3O$: C, 45.2; H, 6.10; N, 4.58. Found: C, 45.3; H, 6.00; N, 4.91. A better yield (2.95 g, 89%) was obtained when using CH_2Cl_2 as solvent.

(20) Higashi, T. *ABSCOR−An Empirical Absorption Correction Based on Fourier Coefficient Fitting*; Rigaku Corporation: Tokyo, 1995.
(21) Sheldrick G. M. *SHELXL PC Manual*; Siemens Analytical X-ray Instruments, Inc.: Madison, WI, 1990.
(22) Sheldrick, G. M. *SHELXL-93*, A program for crystal structure refinement; University of Göttingen, 1993.

[Zr{N(SiMe$_3$)C(Ph)C(SiMe$_3$)(C$_9$H$_6$N-2)}Cl$_3$] (5d). To a suspension of $ZrCl_4$ (0.39 g, 1.67 mmol) in CH_2Cl_2 (25 mL) was added **5b** (1.53, 1.63 mmol). After stirring for 16 h the orange mixture was filtered and the filtrate concentrated to ca. 10 mL. Cooling to −30 °C afforded yellow crystals of **5d** (0.81 g). Concentration of the mother liquor gave a second crop. Total yield: 1.10 g (1.87 mmol, 57%). Anal. Calcd for $C_{23}H_{29}N_2Si_2ZrCl_3$: C, 47.0; H, 4.98; N, 4.77. Found: C, 46.8; H, 4.86; N, 4.86. MS (EI, 70 eV): *m*/*z* 586 (16, M^+), 571 (34, $(M - Me)^+$), 551 (8, $(M - Cl)^+$).

[Zr{N(SiMe$_3$)C(Ph)C(SiMe$_3$)(C$_9$H$_6$N-2)}{N(SiMe$_3$)C(Ph)C(SiMe$_3$)(PhCH$_2$-4-C$_9$H$_6$N-2)}Cl] (5e). To a solution of **5b** (0.50 g, 0.53 mmol) in Et_2O (30 mL) at −70 °C was added $PhCH_2MgCl$ (0.95 mL, 0.52 mmol of a 0.547 M solution in Et_2O). The reaction mixture was allowed to reach room temperature; a further portion of the Grignard solution (1.0 mL, 0.55 mmol) was added. The mixture was stirred for another 16 h. Volatiles were removed in a vacuum, and the residue was extracted with hexane (2 × 35 mL). Crystallization at −30 °C afforded **5e** (0.26 g, 0.26 mmol, 50%) as an orange material. ^{1}H NMR (360 MHz, benzene-d_6): δ 8.65 (d, J = 8.3 Hz, 1H, 9-qui), 8.03 (d, J = 6.6 Hz, 1H, 9-qui), 7.57 (m, 2H), 7.33−7.10 (m and C_6D_5H), 6.89 (t, J = 7.3 Hz, 1H), 6.49 (d, J = 7.8 Hz, 1H), 6.38 (t, J = 7.3 Hz, 1H), 6.06 (t, J = 6.8 Hz, 1H), 5.83 (d, J = 8.1 Hz, 1H), 4.84 (d, J = 5.0 Hz, 1H, NC=C(H)), 3.99 (X part of ABX pattern, 1H, C(*H*)(CH_2Ph)), 3.01 (AB part of ABX pattern, J_{AB} = 13 Hz, 2H, C(H)(C*H*$_2$Ph)), 0.42 (s, $SiMe_3$), 0.25 (s, $SiMe_3$), −0.03 (s, $SiMe_3$), −0.12 ($SiMe_3$). ^{13}C NMR (75.4 MHz, benzene/benzene-d_6): δ 49.4 (*C*(H)(CH_2Ph), 41.9 (C(H)(*C*H$_2$Ph), 3.9 ($SiMe_3$), 2.7 ($SiMe_3$), 2.5 ($SiMe_3$), 1.1 ($SiMe_3$). Anal. Calcd for $C_{53}H_{65}ClN_4Si_4Zr$: C, 63.8; H, 6.57; N, 5.62. Found: C, 64.0; H, 6.68; N, 5.74. MS (EI, 70 eV): *m*/*z* 995 (0.9, M^+), 960 (0.2, $(M - Cl)^+$), 905 (13, $(M - CH_2Ph)^+$), 481 (37, [{N(SiMe$_3$)C(Ph)C(SiMe$_3$)(PhCH$_2$-4-C$_6$H$_9$N-2)}H]$^+$), 389 (58, [N(SiMe$_3$)C(Ph)C(SiMe$_3$)(C$_6$H$_9$N-2)]$^+$).

EHMO Calculations. Extended Hückel calculations were carried out using the CACAO software package with the standard parameter set as supplied with the program (weighted H_{ij} formula).[23] Idealized C_2 symmetrical models **A** and **B** were constructed using the (averaged) bonding parameters of the X-ray structures of **2b** and **3b**, respectively. Other parameters used were Zr−H = 1.9 Å, N−H = 1.07 Å, C−H = 1.09 Å, Zr−Cp = 2.2 Å, Cp-Zr−Cp = 130°, and H−Zr−H = 95°.

Ethylene Polymerization. In a typical experiment **5d** (31 mg, 0.053 mmol) was dissolved in a solution of MAO in toluene (10% (w/w), 3.5 mL, 5.4 mmol of Al). The solution was then diluted with toluene (31.5 mL) and degassed, and ethylene (1 bar) was admitted to the stirred reaction mixture. After 30−180 min, the polymerization reaction was quenched with a 10:1 mixture of MeOH and HCl (1 M). The solid polymer was isolated, washed succesively with HCl (1 M), water, and MeOH, and dried at 80 °C to constant weight (usually 24 h).

1-Hexene Polymerization. To **3d** (32.0 mg, 59.5 μmol), dissolved in a solution of MAO (10% (w/w) in toluene, 5.60 mL, 8.7 mmol of Al), was added 1-hexene (10.0 mL, 80.0 mmol). The red solution, which turned brown slowly, was stirred for 25 h and then quenched with MeOH/HCl (1 M). The water layer was separated and extracted with toluene (35 mL). The combined toluene layers were washed with water (2 × 25 mL) and dried ($MgSO_4$). Volatiles were removed in a vacuum (40 °C, 0.001 mbar), affording a yellow oil. Yield: 0.20 g. ^{1}H NMR end-group analysis (300 MHz, chloroform-d_1): δ 5.80 (m, 1H, CH_2=C(*H*)CH_2R), 5.37−5.34 (RC(*H*)=C(*H*)R′), 5.01−4.90 (m, 2H, C*H*$_2$=C(H)CH_2R), 4.72−4.56 (4 × s, C*H*$_2$=C(R)R′). ^{13}C NMR (75.4 MHz, chloroform-d_1): δ 133.4−125.3 (internal double bond end-groups), 40.21, 34.59, 32.35, 28.70, 23.23, 14.19; resonances due to vinylidene and allyl end-groups not observed due to low intensity.

Ethylene/1-Hexene Copolymerization. 1-Hexene (10.0 mL, 80.0 mmol) dissolved in a solution of MAO ((10% (w/w) in toluene, 3.0 mL, 4.7 mmol of Al) was added to a mixture of **3d** (4.6 mg, 8.5 μmol) and MAO (10% (w/w) in toluene, 0.50 mL, 0.76 mmol of Al) and then pressurized with ethylene (p = 1.5 bar). After ca.1 h the polymerization reaction was quenched with a 10:1 mixture of MeOH in aqueous HCl (1 M), and solid polymer was isolated and washed with successively HCl (1 M), water, and MeOH. Drying (80 °C, 24 h) afforded the polymer (23 mg). The toluene layer was washed with water (2 × 10 mL) and dried ($MgSO_4$). Volatiles were removed in a vacuum (40 °C, 0.001 mbar), affording a colorless wax (10 mg). ^{1}H NMR end-group analysis of the toluene-soluble fraction (300 MHz, chloroform-d_1): δ 5.70 (m, 1H, CH_2=C(*H*)CH_2R), 5.32−5.28 (RC(*H*)=C(*H*)R′), 4.95−4.84 (m, 2H, C*H*$_2$=C(H)CH_2R), 4.66−4.59 (3 × s, C*H*$_2$=C(R)R′).

Acknowledgment. We thank the European Community for a Human Capital and Mobility Grant for B.-J.D., Hong Kong Research Grant Council for a Earmarked Grant CUHK 317/96P, Dr. Ali Abdul-Sada for MS measurements, and BASF for the generous supply of high-purity ethylene and propylene and for analysis of polymer samples.

Supporting Information Available: Listings of all final refined and all calculated atomic coordinates, anisotropic thermal parameters, and a complete list of bond lengths and angles for the X-ray crystallographic structure determinations of **2b**, **2c**, and **3b** can be found in the Supporting Information. This material is available free of charge via the Internet at http://pubs.acs.org.

OM980850B

(23) CACAO for the PC, version 4.0: Mealli, C.; Proserpio, D. M. *J. Chem. Educ.* **1990**, *67*, 399.